

The impact of charge compensated and uncompensated strontium defects on the stabilization of the ferroelectric phase in HfO₂

Robin Materlik,^{1,2} Christopher Künneth,^{1,2} Thomas Mikolajick,^{3,4} and Alfred Kersch^{1, a)}

¹⁾*Department of Applied Sciences and Mechatronics, Munich University of Applied Sciences, Lothstr. 34, 80335 Munich, Germany*

²⁾*These two authors contributed equally to this work.*

³⁾*NaMLab gGmbH, Noethnitzer Strasse 64, 01187 Dresden, Germany*

⁴⁾*Chair of Nanoelectronic Materials, Technische Universität Dresden, Noethnitzer Strasse 64, 01187 Dresden, Germany*

(Dated: 28 August 2017)

Different dopants with their specific dopant concentration can be utilized to produce ferroelectric HfO₂ thin films. In this work it is explored for the example of Sr in a comprehensive first-principles study. Density functional calculations reveal structure, formation energy and total energy of the Sr related defects in HfO₂. We found the charge compensated defect including an associated oxygen vacancy Sr_{Hf}V_O to strongly favour the non-ferroelectric, tetragonal P4₂/mnc phase energetically. In contrast, the uncompensated defect without oxygen vacancy Sr_{Hf} favours the ferroelectric, orthorhombic Pca2₁ phase. According to the formation energy the uncompensated defect can form easily under oxygen rich conditions in the production process. Low oxygen partial pressure existing over the lifetime promotes the loss of oxygen leading to V_O and, thus, the destabilization of the ferroelectric, orthorhombic Pca2₁ phase accompanied by an increase of the leakage current. This study attempts to fundamentally explain the stabilization of the ferroelectric, orthorhombic Pca2₁ phase by doping.

This article may be downloaded for personal use only. Any other use requires prior permission of the author and AIP Publishing. The following article appeared in Appl. Phys. Lett., vol. 111, no. 8, p. 82902, 2017 and may be found at <http://dx.doi.org/10.1063/1.4993110>.

Keywords: ferroelectric, HfO₂, strontium, doping, phase stability, DFT, formation energy, charge

^{a)}Electronic mail: alfred.kersch@hm.edu

Polycrystalline HfO₂ thin films produced by Atomic Layer Deposition (ALD) or Chemical Solution Deposition (CSD) can exhibit ferroelectric properties if they are appropriately doped¹⁻⁹. An orthorhombic, non-centrosymmetric phase (Pca2₁) has been proposed as the source of these properties which has since been confirmed by electron diffraction study¹⁰. Furthermore, another theoretically proposed ferroelectric Pmn2₁ phase has been ruled out by the same study and is therefore not included in this work. Pure HfO₂ occurs naturally in a monoclinic (P2₁/c) phase. With increasing temperature a transformation into the tetragonal (P4₂/mnc) and then the cubic (Fm $\bar{3}$ m) phase occurs¹¹ avoiding the orthorhombic phase. Different Density Functional Theory (DFT) studies consistently calculate the total energy of the orthorhombic phase as second most stable after the monoclinic phase and are able to reproduce the thermally driven phase transformation^{12,13} giving credibility to the used density functionals.

To explain the occurrence of the ferroelectric phenomena, factors favouring the orthorhombic phase have been proposed¹³⁻¹⁵ including entropy contribution, surface or interface energy, stress, and doping. Surface or interface energy stems from the large surface to volume ratio of the individual crystals in the polycrystalline HfO₂ thin films^{13,16} with grain sizes typically in the range of the film thickness (5 nm to 30 nm)¹⁷⁻²⁰. It explains the generally observed decrease or disappearance of the ferroelectric properties with increasing film thickness²¹. For the case of Hf_{1-x}Zr_xO₂, at $x = 0.5$, surface energy or interface energy has been found to be sufficient to explain stability of the orthorhombic phase^{13,16}. For thin films based on pure HfO₂ surface or interface energy is insufficient except for the case of very small grains¹⁷.

In such thin films further stabilization by appropriate doping is required^{7-9,22,23}. For the case of Sr doping, ferroelectricity was observed in a 10 nm film between 1.7 and 7.9 mol% SrO content with the maximum polarization observed at around 3.4 mol% SrO²⁴. The effect of doping on HfO₂ phases has been investigated in earlier works^{25,26} but the Pca2₁ as well as II-valent dopants were not included in the study. The authors found stabilization of the tetragonal phase by IV-valent and stabilization of the cubic phase by III-valent dopants. Due to its II-valent nature, it is expected that each Sr dopant atom is accompanied by an oxygen vacancy for charge compensation. Furthermore, due to opposite charges, the Sr_{Hf}⁻² and V_O⁺² defect should strongly attract each other leading to [Sr_{Hf}V_O]⁰ similar to the case of Mg_{Hf}⁻² or Ba_{Hf}⁻² doping investigated in^{27,28}. However, the defect concentration created during the

manufacturing process is not explicit known and strongly depends on the chemical potential of the defects. In this work the defect notation of Freysoldt et al. is used²⁹.

To propose a consistent scenario for the ferroelectric stability of a Sr doped HfO₂ thin film, we determined total energy and defect formation energy for various defects in monoclinic, orthorhombic, tetragonal and cubic HfO₂ from first principle calculations. These defects include single oxygen vacancies V_O^q with the charges $q = 0, +1, +2$, Sr substituted for Hf with Sr_{Hf}^q ($q = 0, -1, -2$) as well as the compensated defect [Sr_{Hf} V_O]^q ($q = 0, -1, -2$). Oxygen vacancies were placed on the eight next neighboring oxygen sites of a given Sr or Hf atom excluding structural equivalent positions. All shown results always depict the energetically most favourable position. Placing one defect in a 96 or 48 atomic super cell corresponds to a concentration of 3.125 f.u.% (= 1 defect/ 32 formula units) and 6.25 f.u.% (= 1 defect/ 16 formula units) respectively.

DFT calculations were performed using the Local Density Approximation (LDA) and Projector Augmented Wave (PAW)³⁰ Pseudo Potentials (PP) from the GBRV library^{31,32} with the ABINIT code³³⁻³⁵. Several LDA calculations were repeated with the all electron code FHI-AIMS³⁶ based upon numeric, atom-centered orbitals of type tight with first and second tier enabled. In the remainder of this work we will refer to those two methods as plane waves (PW) and numerical orbitals (NO), respectively. The stopping criteria for the electronic convergence was a force criteria of 10⁻⁶ Hartree/Bohr (PW) and 10⁻⁴ eV/Å(NO). The stopping criteria for the structural convergence was a force criteria of 10⁻⁵ Hartree/Bohr (PW) and 10⁻³ eV/Å(NO). Charged and neutral defect calculations in monoclinic, tetragonal, cubic, and orthorhombic HfO₂ were performed with 96 atomic super cells using a 2×2×2 Monkhorst-Pack k-point set, a plane wave cut off of 18 Ha and a PAW cut off of 22 Ha in accordance with a convergence study. Charge neutral 48 atomic super cells with a 2 × 4 × 2 k-point grid were used to determine the phase stability at 6.25 f.u.% defect concentration.

The defect formation energies E_f were calculated as

$$E_f(X, q) = U(X, q) - U(\text{pure}) - \sum_i n_i \mu_i + q(\epsilon_F + \epsilon_{\text{VB}}(\text{pure}) + \Delta V(X, 0)) + E_{\text{Corr}}(X, q) \quad (1)$$

using the DFT total energies U of both HfO₂ without and with a defect $X \in \{\text{Sr}_{\text{Hf}}^q, [\text{Sr}_{\text{Hf}}\text{V}_{\text{O}}]^q, \text{V}_{\text{O}}^q\}$ and charge q . The chemical potential and number of defect atoms of each species is given by μ_i and n_i respectively. The Fermi energy is ϵ_F and the valence band edge is ϵ_{VB} . A

charge correction E_{Corr} with the scaling law³⁷ $E_f \sim a/L + c$ using a 324 atomic super cell and a potential alignment ΔV was applied. a and c are fit parameters and L is the size of the super cell. The chemical potential of Hf was set to the total energy of hcp Hf and of Sr was calculated by the equilibrium condition $\mu_{\text{Sr}} = \mu_{\text{SrO}} - \mu_{\text{O}}$. For the chemical potential of oxygen two cases are considered: oxygen rich and oxygen deficient^{38,39}. In the oxygen rich case μ_{O} is set to $\mu_{\text{O}_2}/2$. Ferroelectric HfO₂ is often deposited on TiN electrodes^{1,2,10,17–20,24,40} which can exist in a partially oxidized state. The oxygen chemical potential μ_{O} for the deficient conditions uses oxygen precipitation into anatase TiO₂. In similar studies²⁸, precipitation into SiO₂ has been used adapting to a Si substrate. Both assumptions, however, lead to very similar formation enthalpies. We therefore calculate $\mu_{\text{O}} = (\mu_{\text{TiO}_2} - \mu_{\text{Ti}})/2$ for the oxygen deficient case.

The main result from this paper is the connection between the phase stability of defective HfO₂ and the conditions under which the defective material can form. FIG. 1 (a) shows the total energy difference ΔU to the monoclinic phase for the Sr_{Hf} defect as a function of the Sr concentration. Both the orthorhombic and tetragonal phase are depicted calculated with PW and NO. The cubic phase turned out to be unstable and is therefore not shown here.

The defect free orthorhombic phase has a ΔU of 53 meV (PW) and 49 meV (NO) while the tetragonal phase has 115 meV (PW) or 114 meV (NO). The Sr_{Hf} defects lead to a decrease of ΔU of about 20 meV for 6 Sr – f.u.% which is roughly the same for both the tetragonal and orthorhombic phase. Therefore, the defect contributes to the stabilization but not sufficiently to fully stabilize the orthorhombic phase on its own. However, according to previous works, in Hf_{1-x}Zr_xO₂^{13,16,41} the surface or interface energy of grains can decrease the energy of the tetragonal and orthorhombic phase below the monoclinic phase and, thus, suppress the formation of the monoclinic phase. The surface or interface energy for the tetragonal and orthorhombic phase are expected to be very similar. Proposing a surface or interface energy penalty for the monoclinic phase is difficult in this case since the issue has not been investigated for doped HfO₂ so far. In Hf_{1-x}Zr_xO₂ considering Zr as a dopant, a typical energy penalty of about 20 meV (for typical grains of 10 nm diameter in a 10 nm film) was found for HfO₂ linearly increasing to about 60 meV for ZrO₂. At the same time the interface energies increased from 174 mJ/m² to 490 mJ/m²¹⁶. There is another argument in favour of a significant increase of the energy penalty for the monoclinic phase with doping. The authors¹⁶ identified the energy penalty with the energy of the tetragonal/monoclinic

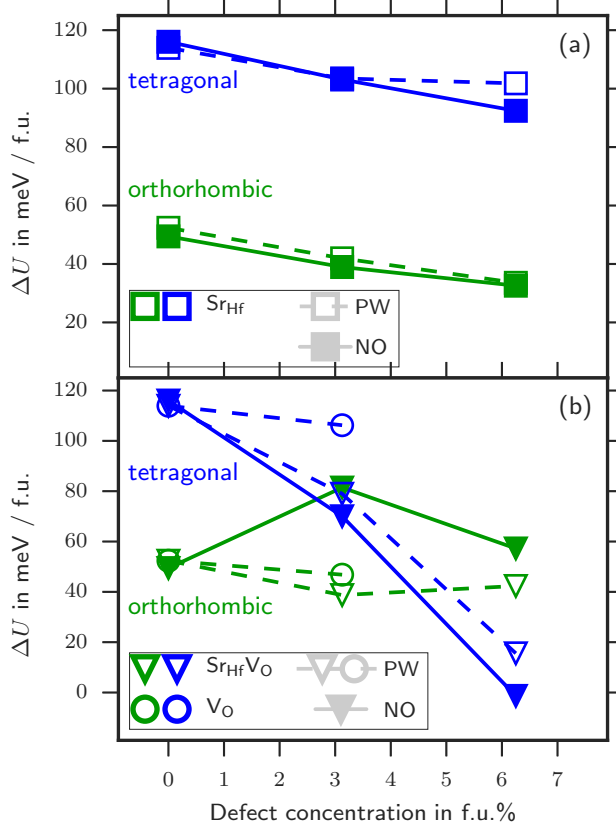


FIG. 1. Defect concentration dependent energy difference $\Delta U = U(o||t) - U(m)$ to the monoclinic phase for the PW (empty symbols, dashed line) and NO (full symbols, continuous line) methodology for the tetragonal (blue) and orthorhombic (green) phase. The different defects are indicated by symbols. (a) shows the vacancy free defects Sr_{Hf} (squares) and (b) shows the vacancy related defects V_O (triangles) and $\text{Sr}_{\text{Hf}}\text{V}_\text{O}$ (circles).

interface observed by Grimley⁴². An interface energy, however, is expected to depend sensitively on doping. Altogether, we expect a surface or interface related energy penalty for the monoclinic phase starting at around 30 meV for pure HfO_2 and increasing significantly with doping. We therefore expect ΔU of the orthorhombic phase to become negative for some Sr concentrations and the film to become ferroelectric. Important for the ferroelectric stabilization is that the orthorhombic phase turns always out to be more favourable than the tetragonal phase.

This is not the case for the compensated defect $[\text{Sr}_{\text{Hf}}\text{V}_\text{O}]^0$ as shown in FIG. 1 (b). The change in ΔU is much larger for the tetragonal phase than for the orthorhombic phase.

Above a threshold of 2 f.u.% to 3 f.u.% (NO) or 5 f.u.% (PW) the material loses ferroelectricity and the tetragonal phase replaces the orthorhombic phase as the most favorable. This would severely limit the dopant concentration range in which ferroelectric properties can be observed and is therefore in conflict with the experimentally observed range for ferroelectricity of 1.7 mol% to 7.9 mol% dopant concentration^{8,24}.

This leads to the question, whether the Sr_{Hf} is indeed always compensated with an oxygen vacancy V_{O} as stoichiometry suggests. An estimation of the vacancy concentration results from an electrical measurement of the leakage current in Sr doped Hf by Pešić et al.⁴⁰, who extracted a vacancy concentration of $5 \times 10^{19} \text{ cm}^{-3}$ which is significantly less than required to pair every Sr atom ($1.4 \times 10^{21} \text{ cm}^{-3}$ for 5 f.u.%) with a vacancy. Crucial for the question, whether Sr_{Hf} or $\text{Sr}_{\text{Hf}}\text{V}_{\text{O}}$ should be expected is the formation energy as a function of the oxygen chemical potential and a kinetic process creating the defect⁴³.

FIG. 2 (a) shows the formation energies under oxygen rich conditions for the orthorhombic phase and for oxygen in the III-valent and IV-valent position. The formation energy does not differ very much from the monoclinic phase (not shown here). The LDA band gap for the orthorhombic phase was found to be 4.41 eV (3.98 eV for the monoclinic and 4.56 eV for the tetragonal). The individual formation energy of charged $\text{Sr}_{\text{Hf}}^{-2}$ and V_{O}^{+2} defects is lower than the formation energy of the combined charge neutral $[\text{Sr}_{\text{Hf}}\text{V}_{\text{O}}]^0$ defect. This might lead to a separated creation of $\text{Sr}_{\text{Hf}}^{-2}$ and V_{O}^{+2} . However, since vacancies are very mobile, the positively charged vacancies V_{O}^{+2} combine with the negatively charged $\text{Sr}_{\text{Hf}}^{-2}$ creating $[\text{Sr}_{\text{Hf}}\text{V}_{\text{O}}]^0$ with an energy release of 2.36 eV. Under oxygen rich conditions, few $\text{Sr}_{\text{Hf}}\text{V}_{\text{O}}$ are expected in the end except close to the interface where some oxygen loss towards the electrode has to be expected. As a result, a film with substitutional Sr_{Hf} defects and few compensated defects is expected, but at the electrode interface a significant amount of compensated $\text{Sr}_{\text{Hf}}\text{V}_{\text{O}}$ defects is possible which may stabilize a tetragonal interlayer⁴² and may be a prerequisite of the energy penalty to suppress the monoclinic phase. This would support the assumptions made by Pešić⁴⁰. The acceptor doping without charge compensation achieved under oxygen rich conditions is often desired to improve electric isolation since the negative space charge increases the band offset to the electrode.

During the life time of a ferroelectric HfO_2 stack, the external oxygen partial pressure is defined by the oxidized electrodes. FIG. 2 (b) shows the formation energy under such oxygen deficient conditions. As there is no new Sr-source, only vacancies can be created possibly due

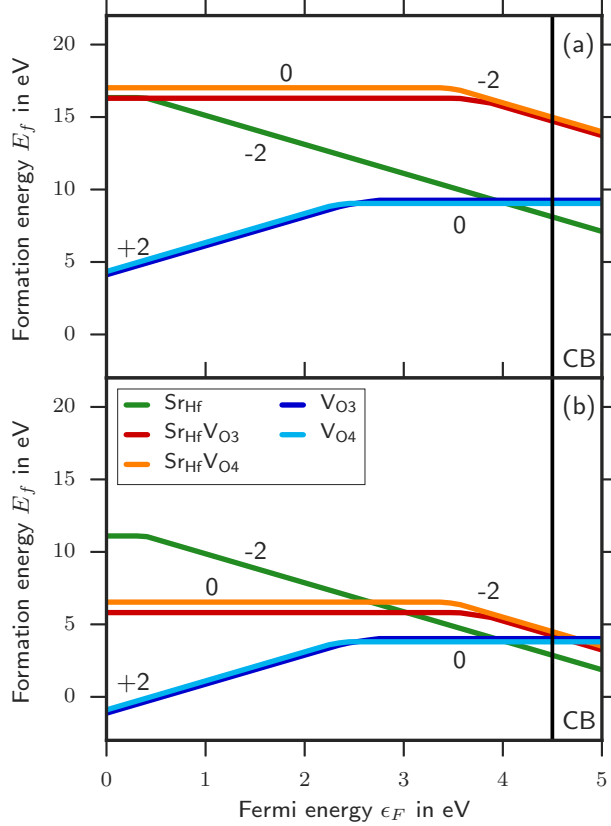


FIG. 2. Figure 2 shows the formation energies of the orthorhombic phase for (a) oxygen rich and (b) oxygen deficient conditions, respectively. The formation energies are calculated by EQ. 1 and the charge states are indicated by numbers. The values are not scaled to the experimental band gap and CB marks the LDA-DFT calculated conduction band.

to field cycling. Since the energy of $[\text{Sr}_{\text{Hf}}\text{VO}]^0$ is lower than the sum of V_{O}^{+2} and $\text{Sr}_{\text{Hf}}^{-2}$, these vacancies will recombine quickly with the already present substitutional Sr defects leading to a charge compensation. The concentration of $\text{Sr}_{\text{Hf}}^{-2}$ will decrease and that of $[\text{Sr}_{\text{Hf}}\text{VO}]^0$ will increase. The implication on the phase stability is a gradual degradation of the orthorhombic phase content accompanied by a decrease of the remanent polarization. A further implication concerning the electron transport is that the charge transition level of a deep defect state promotes trap assisted tunneling (TAT). The related charge transition levels $\epsilon(0/-1) = 3.63\text{ eV}$ and $\epsilon(-1/-2) = 3.92\text{ eV}$ close to the conduction band release electrons which modify the space charge and contribute to TAT. Therefore, a moderate increase of leakage current with time would be expected indicating an increase of charge compensated defects.

As the creation of $\text{Sr}_{\text{Hf}}\text{V}_{\text{O}}$ under oxygen deficient conditions is preferred, the concentration of V_{O} will stay on a relatively low level and constant over time. However, the V_{O} defects with charge transition levels at $\epsilon(+2/+1) = 2.41$ eV and $\epsilon(+1/0) = 2.81$ eV are about 2 eV below the conduction band and, therefore, can be occupied by tunneling electrons promoting leakage current.

A last argument explains why the Sr_{Hf} defect favors the orthorhombic and $\text{Sr}_{\text{Hf}}\text{V}_{\text{O}}$ defect the tetragonal phase in total energy. The cause for the stabilization of the orthorhombic and tetragonal phase by Sr_{Hf} defects can be found in the bond length of the Sr atom to its neighboring oxygen atoms. Calculations of SrO and SrO_2 show a bond length between 2.53 and 2.60 Å, respectively. In undoped HfO_2 the average bond length is 2.12 Å for the monoclinic and orthorhombic phase and 2.17 Å for the tetragonal phase. Substituting a Sr atom on a Hf site, the bond length increases to only 2.35 Å for the monoclinic phase but to 2.37 Å for the orthorhombic and tetragonal phase. Sr in monoclinic HfO_2 is therefore energetically more unfavourable than in the orthorhombic or tetragonal phase, therefore the energy difference to the monoclinic phase decreases with doping. Introducing vacancies, the monoclinic average bond length increases to 2.38 Å, but the tetragonal value of 2.47 Å almost matches the value of SrO and is accompanied by the significant decrease in total energy difference, see FIG. 1.

In summary a mechanism is proposed, based on first-principles DFT calculations, to explain the influence of Sr doping on the phase stability in HfO_2 . The tetragonal phase is strongly preferred by the incorporation of the $\text{Sr}_{\text{Hf}}\text{V}_{\text{O}}$ defects while the Sr_{Hf} allows for the stabilization of the ferroelectric orthorhombic phase. The uncompensated defect can form in sufficiently oxygen rich environments, which might exist during the production process. The loss of oxygen during field cycling may increase the charge compensation which promotes the phase transformation into other HfO_2 polymorphs. This contributes to the fatigue behavior. The proposed mechanism has the potential to describe the action of other dopants on the ferroelectric phase in HfO_2 if appropriately adapted and expanded.

The author wants to thank U. Schröder, T.Schenk, Min Hyuk Park from NamLab/SNU, and U. Böttger and S. Starschich from RWTH Aachen for discussions. The German Research Foundation (Deutsche Forschungsgemeinschaft) is acknowledged for funding this research in the frame of the project Inferox (Project No. MI 1247/111). The authors gratefully acknowledge the Gauss Centre for Supercomputing e.V. (www.gauss-centre.eu) for funding

this project by providing computing time on the GCS Supercomputer SuperMUC at Leibniz Supercomputing Center (LRZ, www.lrz.de).

REFERENCES

- ¹T. S. Böске, J. Müller, D. Bräuhaus, U. Schröder, and U. Böttger, “Ferroelectricity in hafnium oxide thin films,” *Applied Physics Letters* **99**, 102903 (2011), <http://dx.doi.org/10.1063/1.3634052>.
- ²J. Müller, T. S. Böске, U. Schröder, S. Mueller, D. Bräuhaus, U. Böttger, L. Frey, and T. Mikolajick, “Ferroelectricity in simple binary zro2 and hfo2,” *Nano Letters* **12**, 4318–4323 (2012), PMID: 22812909, <http://dx.doi.org/10.1021/nl302049k>.
- ³M. H. Park, H. J. Kim, Y. J. Kim, W. Lee, H. K. Kim, and C. S. Hwang, “Effect of forming gas annealing on the ferroelectric properties of hf0.5zr0.5o2 thin films with and without pt electrodes,” *Applied Physics Letters* **102**, 112914 (2013), <http://dx.doi.org/10.1063/1.4798265>.
- ⁴P. D. Lomenzo, Q. Takmeel, C. Zhou, Y. Liu, C. M. Fancher, J. L. Jones, S. Moghadam, and T. Nishida, “The effects of layering in ferroelectric si-doped hfo2 thin films,” *Applied Physics Letters* **105**, 072906 (2014), <http://dx.doi.org/10.1063/1.4893738>.
- ⁵T. Shimizu, K. Katayama, T. Kiguchi, A. Akama, T. J. Konno, O. Sakata, and H. Funakubo, “The demonstration of significant ferroelectricity in epitaxial y-doped hfo2 film,” *Scientific Reports* **6** (2016), 10.1038/srep32931, <http://dx.doi.org/10.1038/srep32931>.
- ⁶S. Starschich, T. Schenk, U. Schroeder, and U. Boettger, “Ferroelectric and piezoelectric properties of hf1-xzrxo2 and pure zro2 films,” *Applied Physics Letters* **110**, 182905 (2017), <http://dx.doi.org/10.1063/1.4983031>.
- ⁷M. H. Park, Y. H. Lee, H. J. Kim, Y. J. Kim, T. Moon, K. D. Kim, J. Müller, A. Kersch, U. Schroeder, T. Mikolajick, and C. S. Hwang, “Ferroelectricity and antiferroelectricity of doped thin hfo2-based films,” *Advanced Materials* **27**, 1811–1831 (2015).
- ⁸U. Schroeder, E. Yurchuk, J. Müller, D. Martin, T. Schenk, P. Polakowski, C. Adelman, M. I. Popovici, S. V. Kalinin, and T. Mikolajick, “Impact of different dopants on the switching properties of ferroelectric hafniumoxide,” *Japanese Journal of Applied Physics* **53**, 08LE02 (2014).

- ⁹T. Olsen, U. Schröder, S. Müller, A. Krause, D. Martin, A. Singh, J. Müller, M. Geidel, and T. Mikolajick, “Co-sputtering yttrium into hafnium oxide thin films to produce ferroelectric properties,” *Applied Physics Letters* **101**, 082905 (2012), <http://dx.doi.org/10.1063/1.4747209>.
- ¹⁰X. Sang, E. D. Grimley, T. Schenk, U. Schroeder, and J. M. LeBeau, “On the structural origins of ferroelectricity in hfo₂ thin films,” *Applied Physics Letters* **106**, 162905 (2015), <http://dx.doi.org/10.1063/1.4919135>.
- ¹¹J. Wang, H. P. Li, and R. Stevens, “Hafnia and hafnia-toughened ceramics,” *Journal of Materials Science* **27**, 5397–5430 (1992).
- ¹²T. D. Huan, V. Sharma, G. A. Rossetti, and R. Ramprasad, “Pathways towards ferroelectricity in hafnia,” *Phys. Rev. B* **90**, 064111 (2014).
- ¹³R. Materlik, C. Künneth, and A. Kersch, “The origin of ferroelectricity in hf_{1-x}zr_xo₂: A computational investigation and a surface energy model,” *Journal of Applied Physics* **117**, 134109 (2015), <http://dx.doi.org/10.1063/1.4916707>.
- ¹⁴S. E. Reyes-Lillo, K. F. Garrity, and K. M. Rabe, “Antiferroelectricity in thin-film zro₂ from first principles,” *Phys. Rev. B* **90**, 140103 (2014).
- ¹⁵R. Batra, H. D. Tran, and R. Ramprasad, “Stabilization of metastable phases in hafnia owing to surface energy effects,” *Applied Physics Letters* **108**, 172902 (2016), <http://dx.doi.org/10.1063/1.4947490>.
- ¹⁶C. Künneth, R. Materlik, and A. Kersch, “Modeling ferroelectric film properties and size effects from tetragonal interlayer in hf_{1-x}zr_xo₂ grains,” *Journal of Applied Physics* **121**, 205304 (2017), <http://dx.doi.org/10.1063/1.4983811>.
- ¹⁷P. Polakowski and J. Müller, “Ferroelectricity in undoped hafnium oxide,” *Applied Physics Letters* **106**, 232905 (2015), <http://dx.doi.org/10.1063/1.4922272>.
- ¹⁸M. H. Park, H. J. Kim, Y. J. Kim, Y. H. Lee, T. Moon, K. D. Kim, S. D. Hyun, and C. S. Hwang, “Study on the size effect in hf_{0.5}zr_{0.5}o₂ films thinner than 8nm before and after wake-up field cycling,” *Applied Physics Letters* **107**, 192907 (2015), <http://dx.doi.org/10.1063/1.4935588>.
- ¹⁹M. H. Park, H. J. Kim, Y. J. Kim, W. Lee, T. Moon, and C. S. Hwang, “Evolution of phases and ferroelectric properties of thin hf_{0.5}zr_{0.5}o₂ films according to the thickness and annealing temperature,” *Applied Physics Letters* **102**, 242905 (2013), <http://dx.doi.org/10.1063/1.4811483>.

- ²⁰H. J. Kim, M. H. Park, Y. J. Kim, Y. H. Lee, W. Jeon, T. Gwon, T. Moon, K. D. Kim, and C. S. Hwang, “Grain size engineering for ferroelectric hfo₂ films by an insertion of al₂o₃ interlayer,” *Applied Physics Letters* **105**, 192903 (2014), <http://dx.doi.org/10.1063/1.4902072>.
- ²¹M. Hoffmann, U. Schroeder, T. Schenk, T. Shimizu, H. Funakubo, O. Sakata, D. Pohl, M. Drescher, C. Adelman, R. Materlik, A. Kersch, and T. Mikolajick, “Stabilizing the ferroelectric phase in doped hafnium oxide,” *Journal of Applied Physics* **118**, 072006 (2015), <http://dx.doi.org/10.1063/1.4927805>.
- ²²S. Mueller, J. Mueller, A. Singh, S. Riedel, J. Sundqvist, U. Schroeder, and T. Mikolajick, “Incipient ferroelectricity in al-doped hfo₂ thin films,” *Advanced Functional Materials* **22**, 2412–2417 (2012).
- ²³S. Mueller, C. Adelman, A. Singh, S. Van Elshocht, U. Schroeder, and T. Mikolajick, “Ferroelectricity in gd-doped hfo₂ thin films,” *ECS Journal of Solid State Science and Technology* **1**, N123–N126 (2012), <http://jss.ecsdl.org/content/1/6/N123.full.pdf+html>.
- ²⁴T. Schenk, S. Mueller, U. Schroeder, R. Materlik, A. Kersch, M. Popovici, C. Adelman, S. V. Elshocht, and T. Mikolajick, “Strontium doped hafnium oxide thin films: Wide process window for ferroelectric memories,” in *2013 Proceedings of the European Solid-State Device Research Conference (ESSDERC)* (2013) pp. 260–263.
- ²⁵C.-K. Lee, E. Cho, H.-S. Lee, C. S. Hwang, and S. Han, “First-principles study on doping and phase stability of hfo₂,” *Phys. Rev. B* **78**, 012102 (2008).
- ²⁶D. Fischer and A. Kersch, “Stabilization of the high-k tetragonal phase in hfo₂: The influence of dopants and temperature from ab initio simulations,” *Journal of Applied Physics* **104**, 084104 (2008), <http://dx.doi.org/10.1063/1.2999352>.
- ²⁷N. Umezawa, M. Sato, and K. Shiraishi, “Reduction in charged defects associated with oxygen vacancies in hafnia by magnesium incorporation: First-principles study,” *Applied Physics Letters* **93**, 223104 (2008), <http://dx.doi.org/10.1063/1.3040306>.
- ²⁸N. Umezawa, “Effects of barium incorporation into hfo₂ gate dielectrics on reduction in charged defects: First-principles study,” *Applied Physics Letters* **94**, 022903 (2009), <http://dx.doi.org/10.1063/1.3070534>.
- ²⁹C. Freysoldt, B. Grabowski, T. Hickel, J. Neugebauer, G. Kresse, A. Janotti,

- and C. G. Van de Walle, “First-principles calculations for point defects in solids,” *Rev. Mod. Phys.* **86**, 253–305 (2014).
- ³⁰P. E. Blöchl, “Projector augmented-wave method,” *Phys. Rev. B* **50**, 17953–17979 (1994).
- ³¹K. M. R. Kevin F. Garrity, Joseph W. Bennett and D. Vanderbilt, “GBRV high-throughput pseudopotentials (Website),” Online: <https://www.physics.rutgers.edu/gbrv/>.
- ³²K. F. Garrity, J. W. Bennett, K. M. Rabe, and D. Vanderbilt, “Pseudopotentials for high-throughput dft calculations,” *Computational Materials Science* **81**, 446 – 452 (2014).
- ³³X. Gonze, B. Amadon, P.-M. Anglade, J.-M. Beuken, F. Bottin, P. Boulanger, F. Bruneval, D. Caliste, R. Caracas, M. Ct, T. Deutsch, L. Genovese, P. Ghosez, M. Giantomassi, S. Goedecker, D. Hamann, P. Hermet, F. Jollet, G. Jomard, S. Leroux, M. Mancini, S. Mazevet, M. Oliveira, G. Onida, Y. Pouillon, T. Rangel, G.-M. Rignanese, D. Sangalli, R. Shaltaf, M. Torrent, M. Verstraete, G. Zerah, and J. Zwanziger, “Abinit: First-principles approach to material and nanosystem properties,” *Computer Physics Communications* **180**, 2582 – 2615 (2009), 40 YEARS OF CPC: A celebratory issue focused on quality software for high performance, grid and novel computing architectures.
- ³⁴X. Gonze, F. Jollet, F. A. Araujo, D. Adams, B. Amadon, T. Applencourt, C. Audouze, J.-M. Beuken, J. Bieder, A. Bokhanchuk, E. Bousquet, F. Bruneval, D. Caliste, M. Ct, F. Dahm, F. D. Pieve, M. Delaveau, M. D. Gennaro, B. Dorado, C. Espejo, G. Geneste, L. Genovese, A. Gerossier, M. Giantomassi, Y. Gillet, D. Hamann, L. He, G. Jomard, J. L. Janssen, S. L. Roux, A. Levitt, A. Lherbier, F. Liu, I. Lukaevi, A. Martin, C. Martins, M. Oliveira, S. Ponc, Y. Pouillon, T. Rangel, G.-M. Rignanese, A. Romero, B. Rousseau, O. Rubel, A. Shukri, M. Stankovski, M. Torrent, M. V. Setten, B. V. Troeye, M. Verstraete, D. Waroquiers, J. Wiktor, B. Xu, A. Zhou, and J. Zwanziger, “Recent developments in the abinit software package,” *Computer Physics Communications* **205**, 106 – 131 (2016).
- ³⁵M. Torrent, F. Jollet, F. Bottin, G. Zerah, and X. Gonze, “Implementation of the projector augmented-wave method in the abinit code: Application to the study of iron under pressure,” *Computational Materials Science* **42**, 337 – 351 (2008).
- ³⁶V. Blum, R. Gehrke, F. Hanke, P. Havu, V. Havu, X. Ren, K. Reuter, and M. Scheffler, “Ab initio molecular simulations with numeric atom-centered orbitals,” *Computer Physics Communications* **180**, 2175 – 2196 (2009).

- ³⁷G. Makov and M. C. Payne, “Periodic boundary conditions in ab initio calculations,” *Phys. Rev. B* **51**, 4014–4022 (1995).
- ³⁸C. Tang and R. Ramprasad, “Point defect chemistry in amorphous hfo₂: Density functional theory calculations,” *Phys. Rev. B* **81**, 161201 (2010).
- ³⁹J. Lyons, A. Janotti, and C. V. de Walle, “The role of oxygen-related defects and hydrogen impurities in hfo₂ and zro₂,” *Microelectronic Engineering* **88**, 1452 – 1456 (2011), proceedings of the 17th Biennial International Insulating Films on Semiconductor Conference.
- ⁴⁰M. Pešić, F. P. G. Fengler, L. Larcher, A. Padovani, T. Schenk, E. D. Grimley, X. Sang, J. M. LeBeau, S. Slesazeck, U. Schroeder, and T. Mikolajick, “Physical mechanisms behind the field-cycling behavior of hfo₂-based ferroelectric capacitors,” *Advanced Functional Materials* **26**, 4601–4612 (2016).
- ⁴¹R. C. Garvie, “The occurrence of metastable tetragonal zirconia as a crystallite size effect,” *The Journal of Physical Chemistry* **69**, 1238–1243 (1965), <http://dx.doi.org/10.1021/j100888a024>.
- ⁴²E. D. Grimley, T. Schenk, X. Sang, M. Pešić, U. Schroeder, T. Mikolajick, and J. M. LeBeau, “Structural changes underlying field-cycling phenomena in ferroelectric hfo₂ thin films,” *Advanced Electronic Materials* **2**, 1600173–n/a (2016), 1600173.
- ⁴³P. McIntyre, “Bulk and interfacial oxygen defects in hfo₂ gate dielectric stacks: A critical assessment,” *ECS Trans.* **11**, 235–249 (2007), <http://ecst.ecsdl.org/content/11/4/235.full.pdf>.